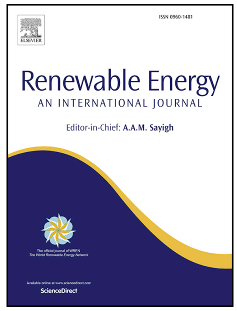

Wave energy harvesting performance of a novel Dual-mode Oscillating Buoy-Parabolic Oscillating Water Column (DOB-POWC) hybrid system

Weifeng Liu, Yong Cheng, Saishuai Dai, Zhiming Yuan, Atilla Incecik

PII: S0960-1481(25)00819-5

DOI: https://doi.org/10.1016/j.renene.2025.123157

Reference: RENE 123157

To appear in: *Renewable Energy*

Received Date: 16 October 2024

Revised Date: 10 April 2025

Accepted Date: 11 April 2025

Wave energy harvesting performance of a novel Dual-mode Oscillating Buoy- Parabolic Oscillating Water Column (DOB-POWC) hybrid system

Weifeng Liu[a], Yong Cheng[a,*], Saishuai Dai[b1], Zhiming Yuan[a, b], Atilla Incecik[b]

[a]*School of naval architecture and ocean engineering, Jiangsu University of Science and Technology, Zhenjiang, 212003, China*

[b]*Naval Architecture, Ocean and Marine Engineering Department, University of Strathclyde, Glasgow, United Kingdom*

Abstract

Incident, reflected, and transmitted wave energies are the primary types of wave energy interacting with marine structures. This paper proposes an innovative hybrid system that integrates an Oscillating Water Column (OWC) device with a cylindrical Oscillating Buoy (OB). The front wall of the OWC is designed with a parabolic shape to collect and focus reflected waves to enhance the power capture performance of the OB device; therefore, it is referred to as the Parabolic Oscillating Water Column (POWC). The OB can harvest energy from both heave and pitch modes and connects to the POWC through a hinge mechanism, known as the Dual-mode Oscillating Buoy (DOB). The proposed DOB-POWC hybrid system can absorb incident wave energy via the DOB, capture transmitted wave energy through the POWC, and converge reflected wave energy within a region using the parabolic wall. Numerical simulations indicate that positioning the DOB at the focal point of the parabolic front wall significantly enhances the capture factor of the hybrid system, with a maximum capture factor reaching 160.63%. Furthermore, the hybrid system combining DOB and POWC features a broad effective bandwidth and can continuously absorb wave energy across a wider range of wave periods, offering a wider capture bandwidth.

Keywords

Oscillating Buoy, Dual-mode motion, Oscillating Water Column, Capture factor, Energy focusing attribute

List of abbreviations：

Nomenclature

Symbols		*Abbreviations*	
b_{pto}	Power Take-Off damping [Nms/rad]	BEM	Boundary Element Method
c	Damping coefficient of PTO [N/(m/s)]	CWR	Capture Width Ratio
D	POWC longitudinal width [m]	DFBI	Dynamics Fluid Body Interaction
d	Distance from the center of DOB to POWC front wall [m]	D-HRWEC	Designed Hinged Raft Wave Energy Converter
d_1	Diameter of DOB [m]	DOB	Dual-mode Oscillating Buoy

[*]Corresponding author. Yong Cheng, Ph.D., mainly research in wave action on maritime structure
E-mail: chengyong@just.edu.cn.

d_2	Draft of DOB [m]	HFC	Horizontal Floating Cylinder
H_i	Incident wave height [m]	OB	Oscillating Buoy
h	Water depth [m]	OWC	Oscillating Water Column
L_1	The length from two ends of the hydraulic piston cylinder to the central hinge point [m]	POWC	Parabolic Oscillating Water Column
T	Wave period [s]	PTO	Power Take-Off
η_{DOB}	Capture factor of DOB [%]	RANS	Reynolds-Averaged Navier-Stokes
η_{POWC}	Capture factor of POWC [%]	VOF	Volume of Fluid
λ	Wavelength [m]	WEC	Wave Energy Converter
		CFD	Computational Fluid Dynamics

1.Introduction

As fossil fuel resources are depleted and the greenhouse effect intensifies, renewable energy is becoming increasingly competitive and gaining greater attention. Wave energy is the most potent and widely distributed form of marine renewable energy, but it has yet to be commercially developed. Its energy density is five times greater than that of wind energy and twenty times greater than that of solar energy [1]. Wave energy offers a longer annual power generation duration compared to wind and solar energy, with substantial reserves estimated at up to 7 billion kilowatts. Although the first patent for wave energy was filed in the early 17th century, wave energy harvesting and utilization remain in the developmental stage due to various challenges. To date, the commercialization of wave energy applications has faced significant challenges. The primary challenges include high installation costs [2] and relatively low energy conversion efficiency, resulting in a higher Levelized Cost of Energy (LCOE) compared to other renewable technologies, such as wind and solar, which diminishes its commercial attractiveness [3]. For wave energy to be deemed an economically viable energy source, substantial improvements in the capture factor are necessary. This paper proposes a new hybrid wave energy harvesting device capable of collecting radiated and reflected waves (waves that do not contribute to energy capture) for power generation, resulting in a high capture factor design.

The Oscillating Water Column (OWC) device is among the most promising Wave Energy Converters (WECs) because it has a limited number of moving parts, all positioned above the water. Having fewer moving parts decreases the likelihood of mechanical failure in wave energy harvesting devices. Compared to other types of WECs, the OWC dissipates excess wave power more effectively, thereby enhancing the capture factor [4]. A substantial proportion of WEC prototypes deployed at sea are of the OWC type [5]. Extensive research has been conducted on OWC devices. Evans [6] initiated theoretical investigations of OWC devices based on linear wave theory, contributing to their widespread adoption. Recent research on OWCs primarily focuses on optimizing hydrodynamic conversion processes. Optimization efforts include studies on front wall entrance geometry [7], chamber shape [8], PTO damping [9] and more. In addition to functioning as a stand-alone marine device [10], the OWC can be integrated with other offshore structures such as monopile foundations [11], breakwaters [12] and floating offshore wind turbine [13] etc. The concept of multi-chamber OWC devices was introduced to enhance hydrodynamic efficiency across a broader range of operating conditions [14]. Numerous numerical simulations and experiments demonstrate that multi-chamber designs can significantly enhance the overall power output of OWCs. Zhao et al. [15] conducted experimental studies on the hydrodynamic performance of the multi-chamber OWC-breakwater system. The results indicate that the multi-chamber OWC-breakwater performs better in wave attenuation for longer wavelengths and broadens the effective frequency bandwidth. Furthermore, Zhao et al. [16] theoretically investigated a multi-resonant OWC-breakwater array and found that multiple resonances create several peaks in hydrodynamic efficiency while broadening the effective frequency bandwidth. Numerous additional studies on OWC optimization have emerged recently. Ding et al. [17] investigated the performance and response characteristics of the OWC device with varying air chamber widths. Their results indicate that reducing the air chamber width leads to a stable horizontal plane, thereby eliminating standing waves. Gadelho et al. [18] proposed a dual-chamber OWC equipped with a stepped bottom, designed for land installation. The step located in front of the first OWC chamber enhances the device's energy capture capability. Zhao et al. [19] investigated the hydrodynamic characteristics of rectangular OWC arrays under oblique wave conditions. The theoretical results indicate that oscillating resonance along the coast varies considerably with the incident wave angle; for large incident wave angles, peak efficiency occurs at a lower frequency.

The Oscillating Buoy (OB) WEC operates through heave, pitch, surge, or a combination of these motions. A primary challenge in improving the energy conversion efficiency of WECs is the optimization of the harvesting mode. Employing both heave and surge/pitch for power generation can potentially triple the theoretical maximum capture width, indicating that multi-mode WECs possess greater theoretical potential than their single-mode counterparts. Stansby et al. [20] performed hydrodynamic experiments on a line absorber comprising three cylindrical floats, which permit movement in heave, pitch, and surge. The experiments demonstrated that the multi-mode float achieves a larger capture width over a broad range of wave periods. Following this investigation, Stansby et al. [21] conducted experiments and linear diffraction modeling to optimize the power capture of the three-float line absorber WEC M4. Their findings indicate that optimal power capture occurs when the spacing between the first two floats is at least 1.5 times that of the last two floats. Subsequently, Liao et al. [22] proposed a self-contained, non-causal optimal control framework for the multi-float, multi-mode WEC M4. Numerical simulations indicated that this framework maintains a low computational load. D.R. Lande-Sudall et al. [23] extended this work by incorporating hydrodynamic forces into the dynamic frame method, applying it to cases with 3, 6, and 8 floats in both regular and irregular waves. Results were compared with those obtained using the vector method and experimental measurements, showing close agreement and indicating that this method is more robust and versatile. OB WECs are typically integrated with other marine structures, including breakwaters, platforms, and OWCs, rather than being deployed independently. OWC and OB devices represent two primary types of WECs, and their integration can enhance wave energy extraction efficiency [24]. Cui et al. [25] proposed a hybrid WEC that combines an OWC with an OB hinged to the outer wall of the OWC device. They developed an analytical model based on linear potential flow theory and eigenfunction matching methods. Furthermore, Wan et al. [26] investigated the hydrodynamic characteristics of symmetric and asymmetric floats within a hybrid system, emphasizing wave attenuation and energy extraction performance. Results indicate that asymmetric floating bodies demonstrate a higher Capture Width Ratio (CWR) and improved wave attenuation performance.

Additionally, Rashidi et al. [27] investigated the impact of geometric parameters on hybrid WECs, including OWCs and Horizontal Floating Cylinders (HFCs), in both regular and irregular wave conditions. The findings confirm that the hybrid system is more efficient than individual WECs. However, its performance is less efficient in irregular waves than in regular waves.

Research on the performance of WECs often encounters a bottleneck, as it is challenging to bypass inefficient stages through hydrodynamic improvements. Similar to how a paraboloid reflects light to a focal point, marine structures with a parabolic opening can converge waves to the focal position. Positioning the WEC at the focal point can enhance wave energy capture. Zhang et al. [28] developed a three-dimensional numerical wave flume employing the Boundary Element Method (BEM) to investigate the wave field around the parabolic breakwater. Results indicate that, within a specific wave environment, the wave height at the focal point can surpass four times the incident wave height. Subsequently, Mayon et al. [29] positioned the OWC at the focal point of the parabolic breakwater, achieving a 650% improvement in hydrodynamic efficiency. Mayon et al. [30] then conducted an experimental study, supported by numerical simulations, showing that the wave-to-line conversion efficiency of the laboratory model exceeds 70%. Following this experiment, Mayon et al. [31] subsequently conducted an experimental study, supported by numerical simulations, demonstrating that the wave-to-line conversion efficiency of the laboratory model exceeds 70%. The cumulative hydrodynamic efficiency of the array is lower than that of a single OWC chamber at the focal point but higher than that of an isolated OWC chamber in open sea conditions. Furthermore, the hydrodynamic efficiency of the array is more stable. Moreover, Zhou et al. [32] examined the power amplification effect of the parabolic breakwater on the WEC, as well as the additional wave attenuation effect of the WEC on the breakwater. Results indicate that parabolic breakwaters exhibit similar power amplification effects across various WECs. However, larger flat WECs generate more power and demonstrate a more pronounced shadow effect.

Despite extensive research on OB-OWC hybrid systems, multi-mode OB wave energy converters (WECs) and uniquely shaped OWC coupling systems have received limited attention. Furthermore, altering the OWC's front wall to a parabolic shape and positioning the OB at its focal point represents a novel approach. This study proposes an OB-OWC hybrid systems where the OWC device has a parabolic front wall. The parabolic wall collects and focus wave energy towards a point at where an OB WEC is planned. This hybrid system can significantly enhance energy extraction by minimizing energy dissipation through diffracted, radiated, transmitted and reflected waves as mentioned previously. The effectiveness of the above proposed concept is examined numerically in this study.

The structure of this paper is as follows. Section 2 describes the development of a multi-body hydrodynamic model using the nonlinear mode expansion method in the time domain. The numerical results with convergence analysis are compared with published experimental results in Section 3. Section 4 analyzes the nonlinear numerical results. Finally, conclusions are drawn in Section 5.

2.Numerical model

2.1 DOB-POWC integrated system and numerical model

Fig. 1(a) illustrates the hybrid system, which consists of an OWC device and a dual-mode OB connected to the upper wall of the OWC through an articulated mechanism. The articulated mechanism consists of an "L"-shaped beam fixed to the OWC and an inverted "L"-shaped beam securely attached to the OB. These beams are joined by a central hinge, as depicted in **Fig. 1**. A hydraulic Power Take-Off (PTO) system is positioned between the two beams, with one end connected to the "L" beam and the other end to the inverted "L" beam. When exposed to waves, the relative motion between the OB and the OWC induces rotation of the two beams around the central hinge, thereby activating the hydraulic PTO system and generating power. The front wall of the OWC is parabolic, with the OB positioned at the focal point of the parabola. The OWC consists of three equally divided chambers. This hybrid system, comprising a dual-mode OB and a parabolic OWC, is referred to as the Dual-mode Oscillating Buoy-Parabolic Oscillating Water Column (DOB-POWC) hybrid system.

The key geometric dimensions of the hybrid system are as follows: POWC longitudinal width D, distance from the center of DOB to POWC front wall d, the diameter of DOB d_1, the draft of DOB d_2, the length from two ends of the hydraulic piston cylinder to the central hinge point o L_1 and L_2. The distance from the central hinge point to the front wall of POWC is equal to the distance from the central hinge point to the DOB.

The simulation domain is illustrated in **Fig. 1** (c), which includes the coordinate system for both figures. In the simulations, waves propagate along the positive x-axis, pitch motion is defined as rotation about the y-axis, and heave response occurs along the z-axis. The length of the computational domain in the x-direction is approximately 4 wavelengths, while its width corresponds to the width of the POWC in the y-direction. The hybrid system is located at the right end of the flow field. To analyze the interaction between waves and floating bodies, overlapping grids were created around the DOB. The left and right boundaries of the computational domain are designated as velocity inlets, the top boundary as a pressure outlet, and both the bottom boundary and the floater surface as non-slip walls. The lateral boundaries of the simulation domain in the y-direction are defined as symmetry boundaries.

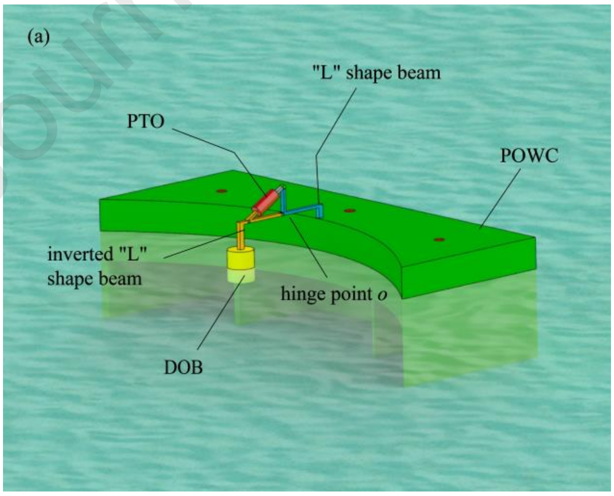

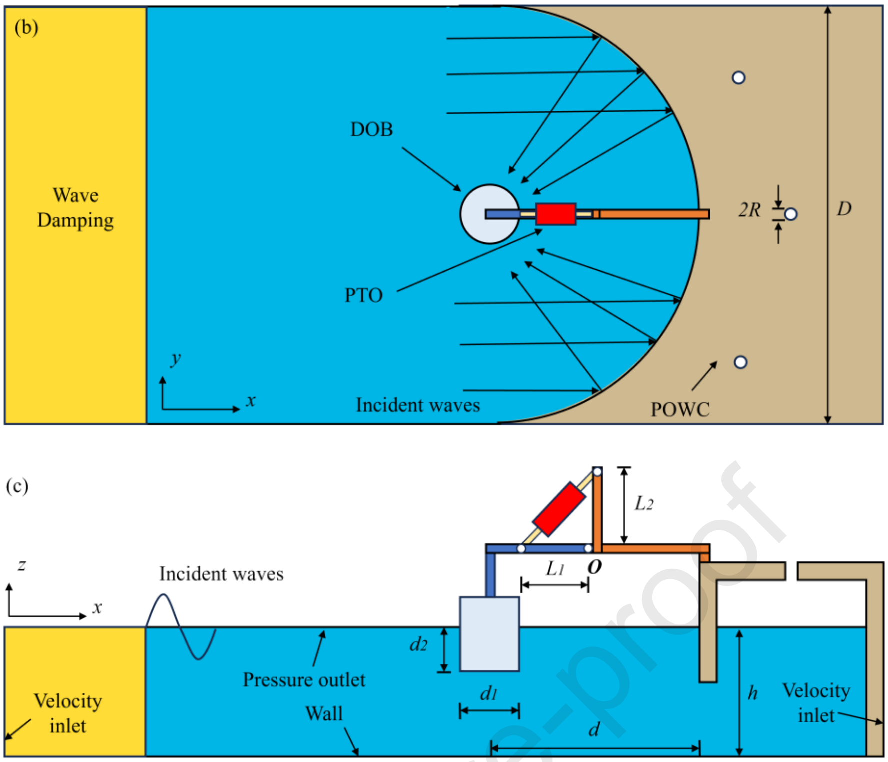

Fig. 1. A diagram of DOB-POWC hybrid system: (a) bird's-eye view (b) Top view (c) Side view.

2.2 Governing equation and wave energy capture factor

In this paper, a three-dimensional numerical wave tank and a hybrid system were constructed using Star CCM+ software to study the interaction between waves and the hybrid system.

The Eulerian multiphase flow model employs the incompressible Reynolds-Averaged Navier-Stokes (RANS) equations to describe water-air mixtures, along with the Volume of Fluid (VOF) method to track the interface between the air and water phases. Fluids in nature are governed by the laws of conservation of mass and momentum. Equation (1) gives the mass conservation equation (also called continuity equation),

$$\frac{\partial \rho}{\partial t} + \nabla \cdot (\rho \boldsymbol{u}) = 0 \tag{1}$$

where t refers to the time, ρ is the fluid density, $\nabla = (\partial / \partial x, \partial / \partial y, \partial / \partial z)$ is the differential operator. For incompressible fluids ρ is constant, and the formula can be abridged as:

$$\nabla \cdot \boldsymbol{u} = 0 \tag{2}$$

The momentum conservation equation can be expressed as:

$$\frac{\partial (\rho \mathbf{v})}{\partial t} + \nabla \cdot \left(\rho \mathbf{v} \cdot \mathbf{v}^{\mathrm{T}} \right) = \nabla \cdot \boldsymbol{\sigma} + \boldsymbol{f}_b \tag{3}$$

where $\boldsymbol{\sigma}$ is the stress tensor, f_b refers to the resultant force of various volume forces acting on the unit volume of the continuum. For fluids, the stress tensor is usually written as the sum of normal stress and shear stress, so $\boldsymbol{\sigma} = -p\boldsymbol{I} + \boldsymbol{T}$. Among them, p is the pressure, $\boldsymbol{T}$ refers to the viscous stress tensor.

The parabolic front wall of POWC can be mathematically described by:

$$y^2 = -2a(x - x_0) \tag{4}$$

where a is a parameter that determines the concavity of the curve around the symmetry axis, and (x, x_0) is the vertex location along the central axis of the parabola. The focal point of the parabola is at (x_f, 0) with $x_f = x_0 - a/2$.

The mechanical coupling between the DOB and the PTO system is established using a Dynamics Fluid Body Interaction (DFBI) model and a mechanical joint module within the software. The PTO system is represented as simplified by applying external damping moments to the DOB. The magnitude of the PTO damping moment [33] can be calculated by:

$$M_{PTO} = \pm \frac{\sqrt{2}}{2} c L_2^{\,2} \dot{\theta} \tag{5}$$

where, the damping coefficient c of PTO is set as 500 (N/(m/s)) [34], the length from the two ends of the hydraulic piston cylinder to the central hinge point is L_1=L_2=0.1m, $b_{pto} = \sqrt{2} c L_2^{\,2} / 2$, $\dot{\theta}$ refers to angular velocity of DOB which is determined by θ(rotation angle of DOB indicated by **Fig. 2**).

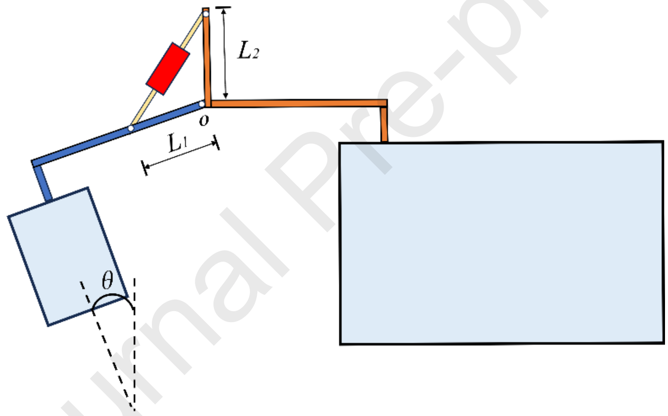

Fig. 2. A diagram of the articulated mechanism with hydraulic energy storage PTO system.

Capture factor is an indicator equivalent to efficiency for WEC power capture performance evaluation, which is defined as the ratio between the captured power E_p to the wave power available to the WEC E_w.

The captured power E_p of DOB can be calculated by:

$$E_p = \frac{1}{2} b_{pto} \omega^2 \Omega^2 \tag{6}$$

where b_{pto} is the PTO damping converted to a rotational damping, for the above PTO model, $b_{pto} = \sqrt{2} c L_2^{\,2} / 2$, ω is the relative rotation frequency, Ω refers to the amplitude of the relative pitch angle between DOB and POWC.

The captured power E_p of POWC can be calculated by:

$$E_p = \frac{1}{mT} \int_0^{mT} q(t) p(t) dt \tag{7}$$

where T refers to incident wave period, $q(t)$ is airflow velocity at the stoma, $p(t)$ is air pressure at the stoma.

The average energy flow rate of unit width E_w' can be calculated by:

$$E_w' = E_w / D_y = \frac{1}{16}\frac{\rho g H_i^2 \omega}{k}\left(1+\frac{2kh}{\sinh 2kh}\right) \quad (8)$$

The average energy flux E_w (with a wave front width equal to the WEC with) of a linear wave can be expressed as:

$$E_w = \frac{1}{16}\frac{\rho g H_i^2 \omega D_y}{k}\left(1+\frac{2kh}{\sinh 2kh}\right) \quad (9)$$

where, ρ refers to the water density, g denotes the acceleration of gravity, H_i refers to the incident wave height, h refers to the water depth, D_y refers to the longitudinal width of the wave energy device and k is the wave number.

The capture factor η can be calculated by:

$$\eta = \frac{E_p}{E_w} \quad (10)$$

The overall capture factor of the DOB-POWC hybrid system can be expressed as:

$$\eta_o = \eta_{\text{PAOWC}} + \eta_{MOB} = \frac{E_{pPAOWC} / D_{yPAOWC} + E_{pMOB} / D_{yMOB}}{E_w'} \quad (11)$$

3 Convergence study and validation

3.1 convergence study

Before evaluating the hydrodynamic performance of the proposed hybrid system, a convergence test for the numerical simulation was performed. The detailed model parameters are provided in **Table 1**. The numerical tank's length and height are set to 4 times the incident wavelength and 2 times the water depth, respectively. A wave forcing damping zone with a length of 1.5 times the incident wavelength is applied at the left end of the tank. The tank height is set to 2 times the water depth. Three different grid schemes (coarse, moderate, and fine) are examined with a wave period of T=1.2s and a wave height of H_i=0.08 m. The detailed mesh parameters are provided in **Table 2**. The time step is fixed at dt=T/1000. The dynamic grid region near the DOB is further refined using a trimmed grid generation to accurately simulate multi-mode motions. **Fig. 3** shows the pitch response time history of the DOB and the pressure response time history inside the POWC chamber for different grid schemes. including the pitch of the DOB and the pneumatic pressure in the POWC chamber. The results indicate that the coarse grid scheme affects numerical accuracy compared to the fine scheme, with differences exceeding 7%. However, the moderate scheme yields results nearly identical to those of the fine scheme within a reasonable computational time, with relative amplitude and phase differences smaller than 5%. The moderate grid scheme and dt=T/1000 are used in Section 4 unless otherwise specified.

Table 1 Key parameters of the numerical model.

Parameters	Value
POWC longitudinal width (D) [m]	5
Distance from the center of DOB to POWC front wall (d) [m]	1.5625
Diameter of DOB (d_1) [m]	0.2
Draft of DOB (d_2) [m]	0.15

Wave height (H_i) [m]	0.08
Water Depth (h) [m]	1
POWC opening ratio (α) [%]	0.625
Damping coefficient of PTO (c) [N/(m/s)]	500
The length from the two ends of the hydraulic piston cylinder to the central hinge point (L_2, L_3) [m]	0.1
Duration of the CFD simulation	10T

Table 2 Mesh parameters

Case	Mesh size(wave)	Mesh size(DOB)
Fine cells	$\Delta z=H_i/20$, $\Delta x=2\Delta z$	$H_i/20$
Moderate cells	$\Delta z=H_i/15$, $\Delta x=2\Delta z$	$H_i/15$
Coarse cells	$\Delta z=H_i/10$, $\Delta x=2\Delta z$	$H_i/10$

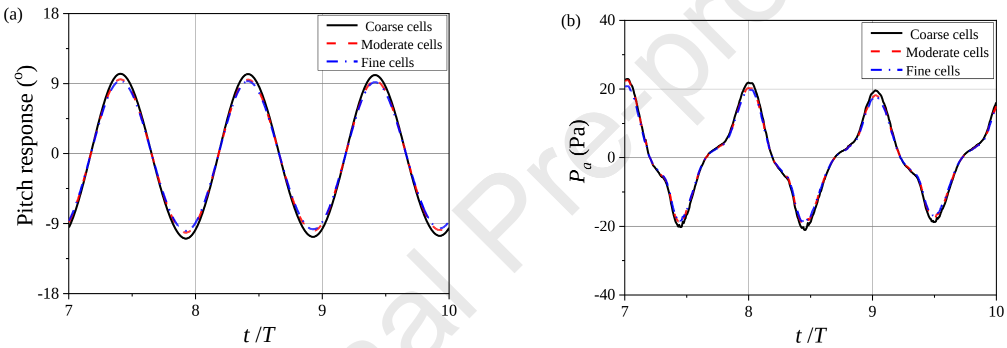

Fig. 3. Mesh convergence of moving responses: (a) the pitch of DOB, (b) pneumatic pressure in the chamber of POWC.

3.2 Validation of DOB

A two-floater hinged raft WEC system, named D-HRWEC, is used to validate the presented DOB numerical model. This WEC system consists of two geometrically identical floaters connected by a hinged arm, along with a controllable PTO unit that provides linear rotational damping of b_{pto}=20 Nms/rad. The experiments corresponding to this system were conducted by Jin et al. [35]. The numerical mesh used for the simulation is shown in **Fig. 4**. The mesh is refined around the free surface and the floaters to ensure accuracy. **Fig. 5** presents a comparison of the relative pitch response between the numerical simulation and Jin's experimental results. The results indicate good agreement between the numerical simulation and the experimental data. The slight over-prediction of numerical values at the trough is likely due to the fact that the physical friction of the controllable PTO mounted inside the WEC device was not included in the numerical simulation.

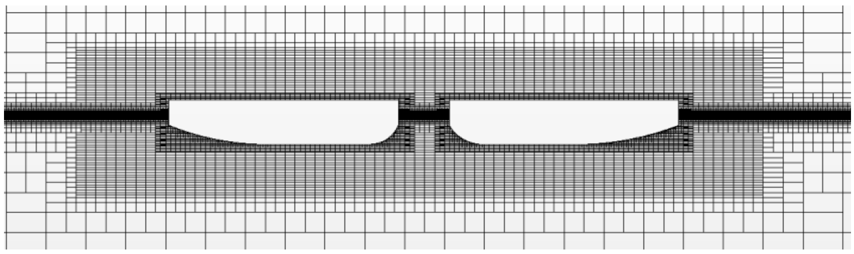

Fig. 4. Mesh generation for the validated model D-HRWEC.

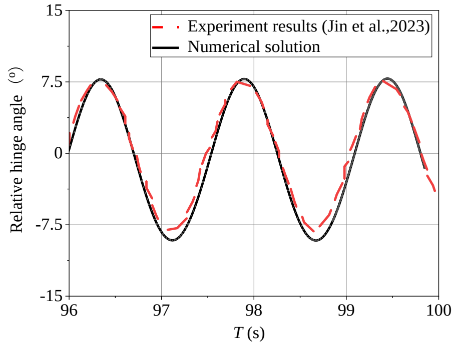

Fig. 5. Numerical and experimental comparison of relative hinge angles between floaters.

3.2 Validation of OWC

In this subsection, the numerical model is verified by reproducing wave interaction with a fixed offshore OWC device. The wave height (H_i) is set as 0.08m and the water depth (h) is 0.6 m. The wave period (T) is 1.3s and the air outlet width (e) is 0.009m. The experiments corresponding to this device were conducted by Iturrioz et al [36]. The numerical mesh used for the simulation is shown in **Fig. 6**. **Fig. 7** presents a comparison of the air pressure between the numerical simulation and Iturrioz's experimental results. The numerical simulation results are in good agreement with the experimental data.

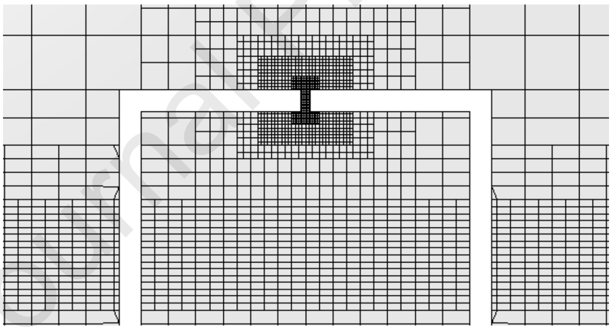

Fig. 6. Mesh generation for the validated model OWC.

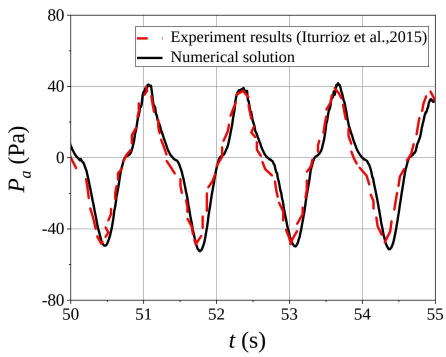

Fig. 7. Numerical and experimental comparison of chamber air pressure.

4 Numerical results

This section presents the numerical simulation results for the proposed hybrid system. First, this section investigates the effects of the parabola's radian and the focal position of the POWC on the hybrid system's capture factor. Following this, an exploration of how the number of chambers impacts the DOB-POWC is conducted. Additionally, this section analyzes the effects of the POWC's opening ratio, the height of the incident waves and the shape of DOB. Unless stated otherwise, the geometric parameters of the DOB-POWC hybrid system align with the data presented in **Table 1**.

4.1 Effect of POWC in different radians

The motion responses of the DOB are heavily dependent on the damping torque generated by the PTO unit. This damping torque, in turn, significantly affects the radiated waves produced by the DOB's motion in waves. The energy dissipation by these radiated waves results in reduced power capture performance. Additionally, varying the radians of the front wall of the POWC results in changes in the focal position. Variations in the gap distance between the DOB and the POWC also significantly impact the overall energy harvesting efficiency of the hybrid system does. Conversely, altering the radian of the POWC's front wall will change both the shape and the width of the POWC chamber. To investigate the above, three different cylindrical gaps from the center of DOB to POWC front wall are considered i.e. d/h=1.3, 1.6 and 2.1, and DOB is placed at the focal position of the parabolic arc. Other parameters are consistent with **Table** 1 in Section 3.1.

Fig. 8 presents the capture factor of DOB (η_{DOB}), POWC (η_{POWC}) and the overall system (η_o) against dimensionless wave period $T(g/h)^{0.5}$. The values from **Fig. 8** (a) show that the maximum capture factor of DOB is enhanced when the gap from the center of DOB to POWC front wall decreased. As can be seen from **Fig. 9**, wave height at the focal point decreased when the gap d/h increased. This explains the phenomenon and indicates that energy is confined within the gap between the DOB and the POWC. When a wave reflects off the floating body, only a small fraction of the energy is radiated outward. Conversely, it is conjectured that the DOB can be approximately considered as isolated devices as the gap distance increases. Because of the wave gathering ability of the parabolic arc front wall, the maximum capture factor of the DOB η_{DOB} can reach 160.63%. In addition, the ability of DOB to harvest long period waves is significantly decreased compared with short period waves. However, as can be seen from **Fig. 8** (b), the capture factor of POWC is enhanced when the dimensionless wave period $T(g/h)^{0.5}$ increased. Therefore, this hybrid system can harvest wave energy effectively in all wave period ($3.1<T(g/h)^{0.5}<6.9$). As shown in **Fig. 8** (b), when the gap d/h increases, the capture factor of POWC decreases. This phenomenon can be explained by the fact that the parabolic arc radian decreases as the gap d/h increases. Consequently, the chamber width of the POWC increases. As the chamber width increases, the water mass within it also increases. As a result, the wave is more readily reflected by the water column, leading to increased energy dissipation. In **Fig. 9**, the position of the maximum wave amplitude is not accurately at the focal point, especially when the focal point is far away from the parabolic wall. This may be due to the actual focus shift caused by the collision of the wave reflected by the parabolic wall with the incident wave.

It is remarkable that the double peak phenomenon would exist in the overall capture factor of the hybrid system which can be seen from **Fig. 8** (c). The phenomenon is more significant when the gap from the center of DOB to POWC front wall decreasing to d/h=1.3. This is due to the fact that the resonance periods of DOB and POWC is different. During short wave periods, the DOB exhibits a higher capture factor, while the POWC is less effective in harvesting wave energy. In contrast, during long wave periods, the POWC has a higher capture factor. Therefore, this hybrid system is capable of harvesting wave energy from both long and short wave periods. The maximum capture factor of the hybrid system will be higher with decreasing the gap *d*/*h*. Additionally, when the gap *d*/*h* increases, the hybrid system can continuously harvest wave energy effectively over a wider range of $T(g/h)^{0.5}$.

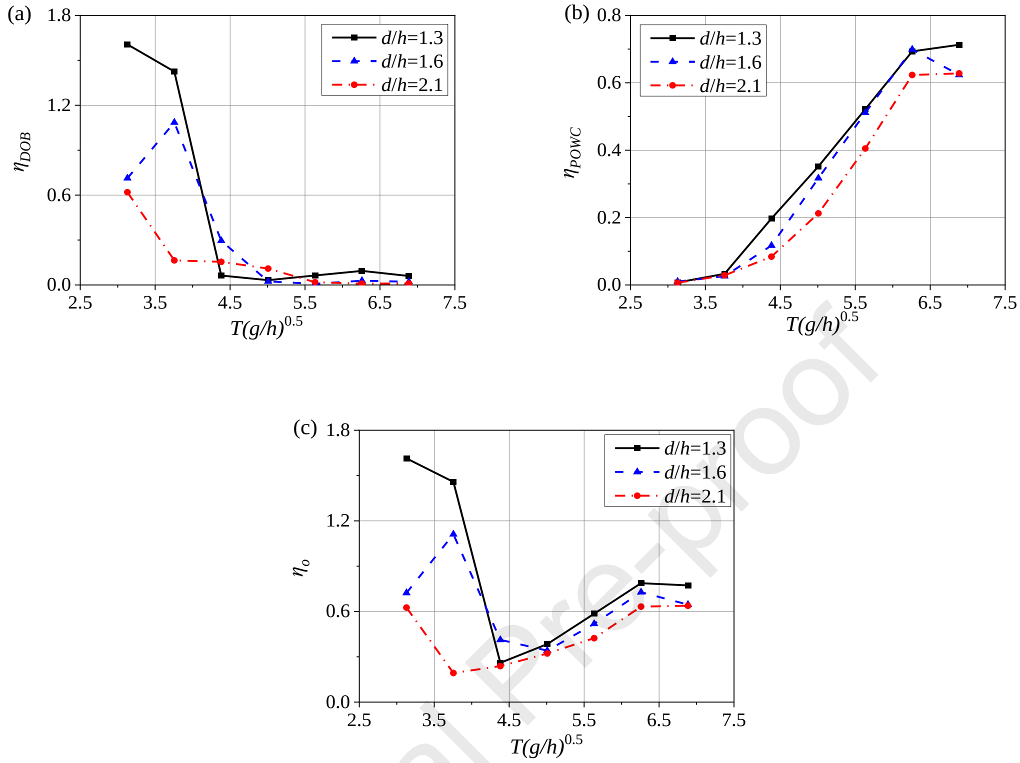

Fig. 8. Capture factor versus nondimensional wave period for different radians of the parabola and the focal position of POWC (a) DOB (b) POWC (c) Overall hybrid system.

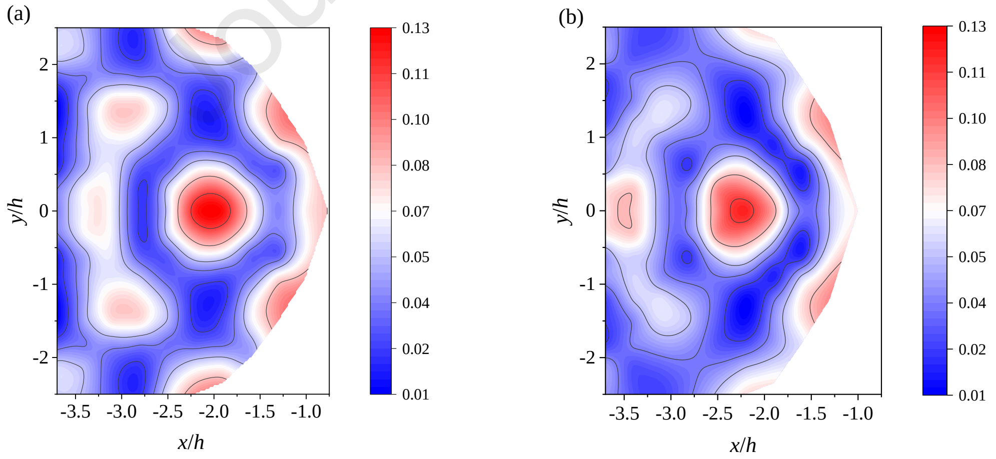

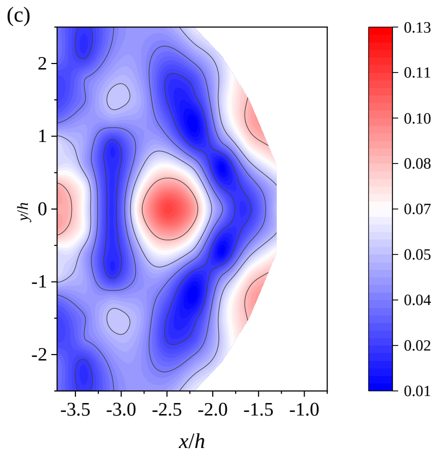

Fig. 9. Wave amplitude around the front wall of POWC ($T(g/h)^{0.5}$=3.8)
(a) d/h=1.3 (b) d/h=1.6 (c) d/h=2.1.

4.2 Effect of the number of POWC chambers

In this paper, the POWC is equipped with three chambers. As the number of chambers will affect the hydrodynamics of the OWCs, the corresponding energy capture performance will be different depending on different number of chambers, leading to different radiation from the OWC device, and hence may impact the performance of the OB device. Therefore, the effect of the number of chambers on the energy conversion of the DOB-POWC hybrid system is discussed in this section. This section considers the different number of POWC chambers i.e. n=1, 2 and 3, and the efficiency contour of the overall system and respective devices is presented in **Fig. 10** (a)-(c).

It is remarkable from **Fig. 10** (a) that the change in the number of POWC chambers has almost no effect on DOB. This phenomenon suggests that variations in wave behavior within the POWC chambers do not influence the wave reflection from the parabolic front wall. Compared with n=2 and 3, n=1 has the largest chamber plane area in which the water column can easily enter to trigger piston-type and sloshing-type resonances, leading to more energy dissipation. In other words, the resonance modes within the chambers are closely linked to the chamber's dimensions relative to the wavelength. This relationship facilitates the alignment of crest and trough regions inside the chamber. Consequently, the opposing liquid levels balance each other out and enhancing overall energy conversion performance of the multi-chamber POWC, as illustrated in **Fig. 10** (b). Moreover, the more chambers the POWC has the better energy harvesting ability for long period waves.

As a comparison, the overall capture factor as presented in **Fig. 10** (c), are found to reach the maximum value 112% at the nondimensional wave period $T(g/h)^{0.5}$=3.8. As the nondimensional wave period $T(g/h)^{0.5}$ continues to increase, the second peak value of capture factor appears. It is clear that the more chambers the POWC has, the higher is the peak value of the capture factor. However, energy conversion is suppressed at the region between the two high regions, generating a 'U' shape area. The wave elevation at various measurement points within the chamber becomes more uniform as the POWC number increases from n=1 to n=3. The performance of the POWC is not significantly affected by the d/h while the performance of the DOB devices in short waves is. This increased uniformity promotes more synchronized pneumatic air movement, resulting in higher wave energy extraction, as shown in **Fig. 11**.

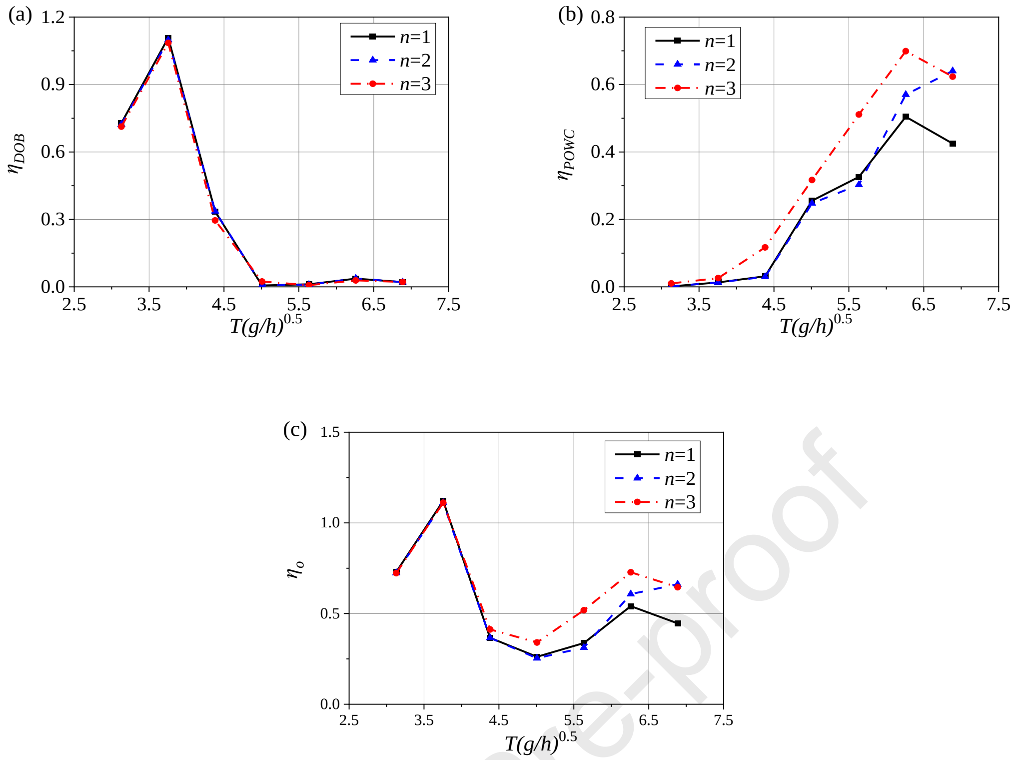

Fig. 10. Capture factor versus nondimensional wave period for different number of POWC chambers (a) DOB (b) POWC (c) Overall hybrid system.

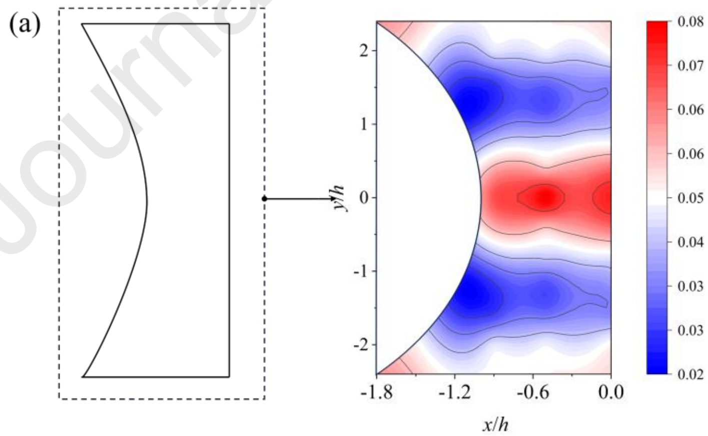

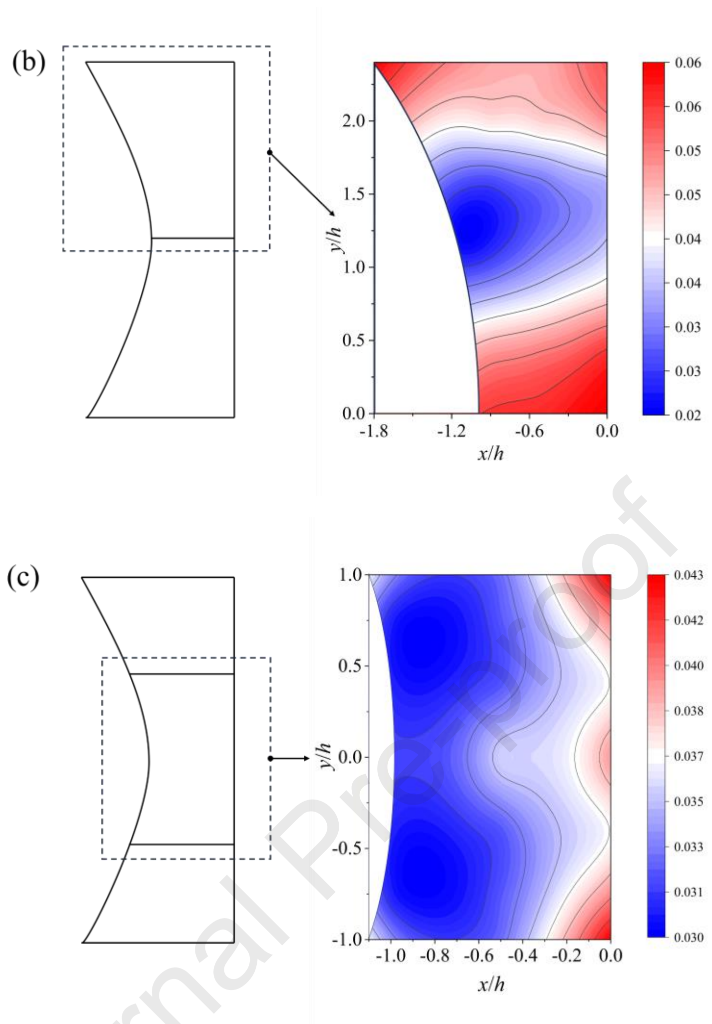

Fig. 11. Wave amplitude of POWC chamber ($T(g/h)^{0.5}$=6.2) (a) n=1 (b) n=2 (c) n=3.

4.3 Effect of the POWC opening ratio

All the simulations above are conducted for a given pneumatic damping coefficient. To further determine the optimal PTO system for the hybrid system, three different pneumatic damping coefficients were tested in this section. In this subsection, three simulation scenarios with opening ratio α=0.625%, 1.25% and 1.875% correspond to pneumatic damping coefficients C_d =68,275, 16,938 and 7470 are performed. **Fig. 12** presents the effects of WECs on the capture factor.

As plotted in **Fig. 12** (a), the capture factor of the DOB remains nearly constant as the opening ratio of the POWC increases. The capture factor of the DOB increases with the opening ratio of the POWC in long wave period ($5<T(g/h)^{0.5}<6.9$). This is because the DOB absorbs energy not captured by the POWC, which is reflected by the back wall. For the POWC, as presented in **Fig. 12** (b), the capture factor decreases with increasing opening ratio. This phenomenon can be explained as follows: When the pneumatic damping coefficient decreases, the water surface elevation in the chamber rises. Looking at **Fig. 12** (a) and (b), it is obvious that the orifice opening ratio has a significant impact on the POWC between 4.5 and 6.5 ($T(g/h)^{0.5}$), meaning the radiated waves within this region will be significantly different, namely, the radiation wave from the OWC to the OB are significantly different under different orifice opening. However, the DOB device is not responding to waves significantly when the wave period exceeds T=4.5. Consequently, the air pressure in the chamber increases, which enhances the wave energy absorption by the POWC. Although the capture factor of POWC changes with the opening ratio, the wave period of the peak value of the capture factor $T(g/h)^{0.5}$=6.3 is invariant, which indicates that the opening ratio will not change the resonance period of POWC. This explains the variation of the overall efficiency with α as displayed in **Fig. 12** (c). In order to enhance the air pressure in the chambers and adequately convert wave energy within rather wider periods, opening ratio α=0.625% is appropriate. Indeed, this is also consistent with the results of Zhao et al. [15], the optimal opening ratio is 0.5-1.0% approximately.

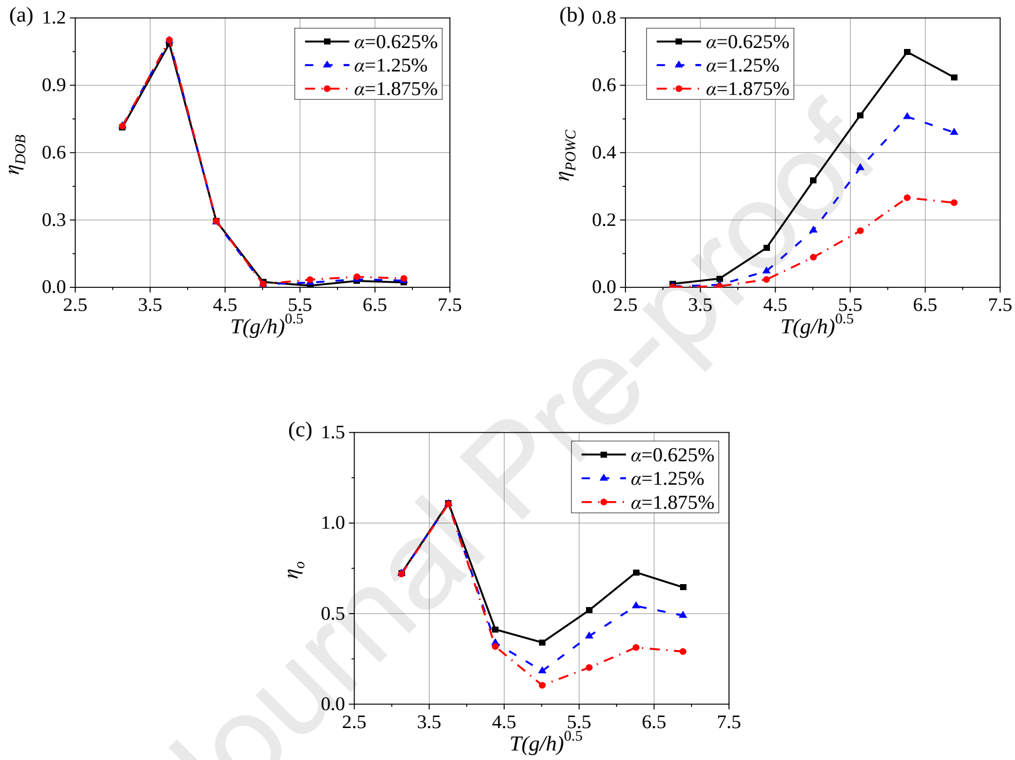

Fig. 12. Capture factor versus nondimensional wave period for different POWC opening ratios (a) DOB (b) POWC (c) Overall hybrid system.

4.4 Effect of different wave heights

The effects of wave height on the hydrodynamic performance of the DOB-POWC integration are examined in this section. The numerical simulations are performed with three different wave heights i.e. H_i/h =0.04, 0.08 and 0.12. Other parameters are maintained the same with the data in **Table 1**. **Fig. 13**(a)–(c) presents the influence of wave height on the capture factor of the DOB, the POWC and the whole hybrid system versus wave period.

As presented in **Fig. 13** (a), when the wave height H_i/h =0.04, $T(g/h)^{0.5}$=3.8, capture factor of DOB occurs a sudden drop. This phenomenon may occur because, under these wave conditions, the peak of the wave reflected from the parabolic front wall coincides with the peak of the incident wave. As a result, the wave forces on the front and back sides of the DOB become balanced, leading to a reduction in the capture factor. Excluding this case, the capture factor of the DOB decreases as the wave height increases. This is expected because short-period waves with high nonlinearity can generate more higher-order waves reflected by the front wall. These higher-order reflected waves are more easily absorbed by the DOB. From **Fig. 13** (b), weaker wave nonlinearity i.e. H_i/h = 0.08 can enhance the maximum capture factor of the POWC compared to H_i/h = 0.04, but it is opposite for stronger wave nonlinearity i.e. H_i/h= 0.12. This implies that a proper POWC design should take into account the change of wave conditions which is important for the resonant characteristic and the operation efficiency, making it relatively rigorous to complete for practical applications. In **Fig. 13** (c), for the DOB-POWC hybrid system, the maximum capture factor (η_o=134.5%) occurs at short period waves. The hybrid system achieves the highest overall energy conversion efficiency when subjected to waves with a height ratio of H_i/h =0.08. This appears to indicate that within all simulated periods, there is a general identity of the maximum overall capture factor for H_i/h =0.08 that the DOB-POWC hybrid system should observe.

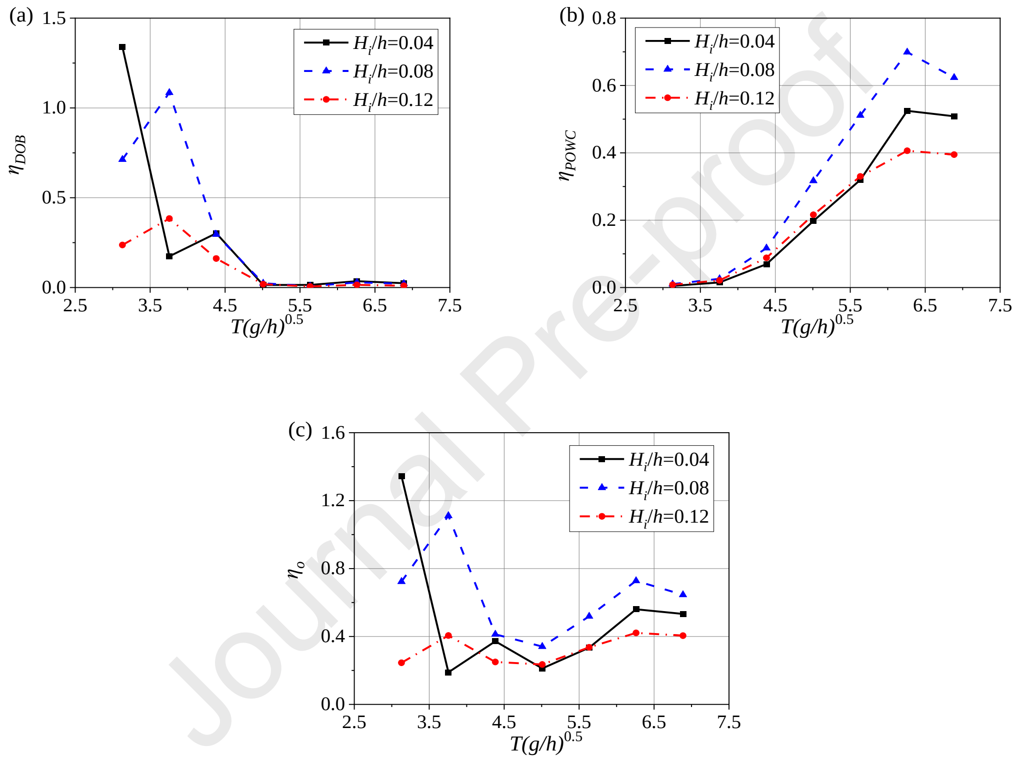

Fig. 13. Capture factor versus nondimensional wave period for different wave heights (a) DOB (b) POWC (c) Overall hybrid system.

4.5 Effect of different DOB shape

The dependence of the energy conversion performance of the integrated system on different DOB shapes is discussed in this section. As indicated in **Fig. 14**, under the condition that the volume and draft of the DOB remain unchanged, the diameter of the DOB is changed to make it show three shapes: slender, medium and flat.

Fig. 15 (a) shows that the DOB's ability to absorb short-period waves improves with increasing diameter. Conversely, slender DOBs exhibit a higher capture factor in the medium wave period ($3.8<T(g/h)^{0.5}<5$). All three DOB shapes are less effective at absorbing long-period waves. In **Fig. 15** (b), all curves of capture factor of POWC exhibit a similar variation trend against the period for different DOB shapes. This behavior occurs because extremely short incident waves are mainly reflected by the DOB, while only moderate and long-period waves can enter the chamber, causing a piston-type oscillatory motion of the water surface. Since the DOB's ability to absorb medium and long-period waves is weak, its shape has minimal impact on the POWC's energy capture.

Fig. 15 (c) displays the capture factor contours for the overall system. The total capture factor curve of the hybrid system mirrors that of the DOB for medium and short-wave periods, indicating that energy harvesting is predominantly influenced by the DOB during these periods. Conversely, in the long-wave period, the total capture factor increases sharply, reflecting the dominance of POWC.

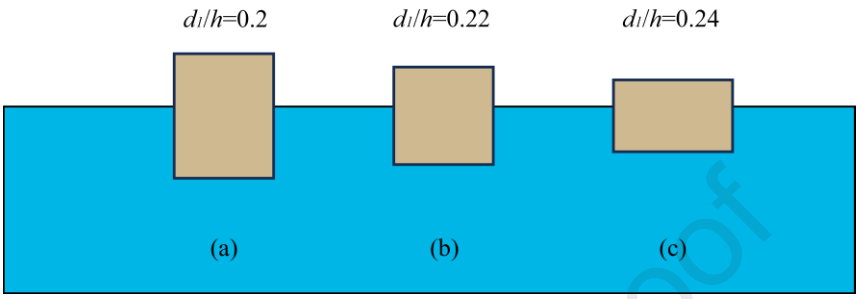

Fig. 14. Schematic diagram of three DOBs with different shapes

(a) d_1/h=0.2 (b) d_1/h=0.22 (c) d_1/h=0.24.

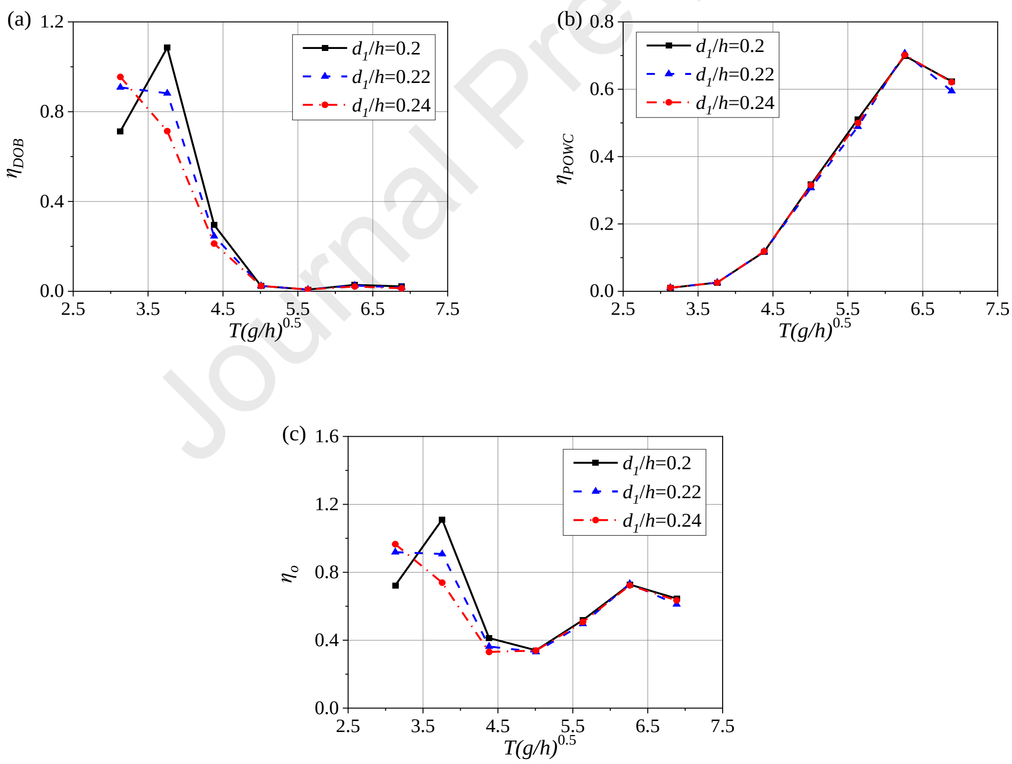

Fig. 15. Capture factor versus nondimensional wave period for different diameter of DOB

(a) DOB (b) POWC (c) Overall hybrid system.

5 Conclusions

This study proposes a hybrid system that integrates a Dual-mode Oscillating Buoy (DOB) hinged to the upper wall of a Parabolic Oscillating Water Column (POWC). An inverted 'L'-shaped beam from the DOB is connected to a rigidly fixed 'L'-shaped beam positioned above the POWC. A PTO unit is installed between the two beams to harness wave energy from the DOB's relative motion in two modes: heave and pitch. This system combines gap resonance between adjacent marine structures with the energy-focusing characteristics of a parabolic front wall. It can harvest incident, reflected, and transmitted wave energies, providing a novel approach to wave energy extraction that has not been previously studied. To demonstrate the high capture factor across a range of broadband periods, a comprehensive hydrodynamic model is developed using a Computational Fluid Dynamics (CFD) algorithm. A moment MPTO is added to the DOB's center of mass to simulate the damping effect of the rigid body in motion. Following a series of systematic simulations, the main conclusions are presented below.

A hybrid system comprising a Dual-mode Oscillating Buoy (DOB) and a Parabolic Oscillating Water Column (POWC) is proposed. The different resonance periods of the DOB and POWC enable the system to continuously and effectively harvest wave energy across a broader range of wave periods.

The unique energy-focusing attribute of a parabolic front wall significantly enhances the capture factor of the DOB-POWC hybrid system, achieving a maximum value of 161.4%. Compared with the ordinary OWC front wall, the parabolic wall can effectively increase the wave height at the focal point and improve the capture factor of WEC at the focal point.

Changing the radian of the POWC's front wall affects the focal position and alters the shape and width of the POWC chamber. Reducing the gap distance between the DOB and POWC enhances the DOB's maximum capture factor and positively impacts the POWC. Generally, a smaller gap distance is more beneficial for overall wave energy conversion.

A multi-chamber POWC performs better in overall energy conversion than a single-chamber POWC. The more chambers the POWC has, the higher the peak capture factor and the wider the harvesting bandwidth.

DOB can absorb energy not captured by the POWC, which is reflected by the back wall. The opening ratio does not affect the resonance period of the POWC. To effectively convert wave energy across a wide range of periods, an opening ratio of α=0.625% is appropriate.

A proper POWC design should consider changes in wave conditions, which are crucial for resonant characteristics and operational efficiency. In this study, a wave height of h=0.08m is deemed appropriate.

Oblate DOBs are more effective at absorbing short-period waves, whereas tenuous DOBs demonstrate higher capture factors for medium and long period waves.

The findings of this study are crucial for improving the design and performance of the OB-OWC integrated system and other marine structures with energy-focusing capabilities. However, the short service life of the DOB presents a significant challenge to its commercialization. Three-dimensional numerical wave tank is used in this paper, but the numerical simulation has some limitations compared with the real situation. Future experiments will further improve the feasibility of the hybrid system. Future research will aim to enhance the stability and longevity of the DOB to improve wave energy collection.

CRediT authorship contribution statement

Weifeng Liu: Validation, Formal analysis, Writing-original draft, Investigation. **Yong Cheng:** Methodology, Software, Data curation, Writing-original draft, Supervision. **Saishuai Dai:** Formal analysis, Data curation, Writing-review & editing, Supervision. **Zhiming Yuan:** Writing-review & editing. **Atilla Incecik:** Supervision.

Declaration of Competing Interest

The authors declare that they have no known competing financial interests or personal relationships that could have appeared to influence the work reported in this paper.

Acknowledgment

The authors are grateful to the National Natural Science Foundation of China (Grant No. 52271278, 52111530137), Natural Science Found of Jiangsu province (Grant No. BK20221389) and the Newton Advanced Fellowships (Grant No. NAF\R1\180304) by the Royal Society for supporting this work.

Reference

[1] López I, Andreu J, Ceballos S, de Alegría IM, Kortabarria I. Review of wave energy technologies and the necessary power-equipment. Renew Sust Energ Rev. 2013;27:413-34.

[2] Cheng Y, Gong J, Zhang J. Hydrodynamic investigation on a single-point moored offshore cage-wave energy converter hybrid system. Ocean Eng. 2024;299:116848.

[3] Shi XL, Li SW, Liang BC, Zhao JC, Liu Y, Wang ZL. Numerical study on the impact of wave-current interaction on wave energy resource assessments in Zhoushan sea area, China. Renew Energy. 2023;215:24.

[4] Rosati M, Henriques JCC, Ringwood JV. Oscillating-water-column wave energy converters: A critical review of numerical modelling and control. Energy Conversion and Management: X. 2022;16:100322.

[5] Falcão AFO, Henriques JCC. Oscillating-water-column wave energy converters and air turbines: A review. Renew Energy. 2016;85:1391-424.

[6] Evans DV. The Oscillating Water Column Wave-energy Device. IMA Journal of Applied Mathematics. 1978;22(4):423-33.

[7] Mandev MB, Altunkaynak A. Cylindrical frontwall entrance geometry optimization of an oscillating water column for utmost hydrodynamic performance. Energy. 2023;280:128147.

[8] Güths AK, Teixeira PRF, Didier E. A novel geometry of an onshore Oscillating Water Column wave energy converter. Renew Energy. 2022;201:938-49.

[9] Cheng Y, Fu L, Dai S, Collu M, Ji C, Yuan Z, et al. Experimental and numerical investigation of WEC-type floating breakwaters: A single-pontoon oscillating buoy and a dual-pontoon oscillating water column. Coastal Engineering. 2022;177:104188.

[10] Liu Z, Xu C, Kim K, Zhang X, Ning D. Hydrodynamic and energy-harvesting performance of an isolated oscillating water column device: An experimental study. Coastal Engineering. 2024;189:104459.

[11] Liu Z, Jin Y, Cao L, Liu G, Guo H. Hydrodynamic performance of an oscillating water column integrated into a hybrid monopile foundation. Ocean Eng. 2024;299:117062.

[12] Didier E, Teixeira PRF. Numerical analysis of 3D hydrodynamics and performance of an array of oscillating water column wave energy converters integrated into a vertical breakwater. Renew Energy. 2024;225:120297.

[13] Zhang D, Chen Z, Liu X, Sun J, Yu H, Zeng W, et al. A coupled numerical framework for hybrid floating offshore wind turbine and oscillating water column wave energy converters. Energy Conversion and Management. 2022;267:115933.

[14] Mia MR, Zhao M, Wu H, Palmer H. Numerical simulation of a stationary offshore multi-chamber OWC wave energy converter. Ocean Eng. 2022;265:112546.

[15] Zhao X, Zhang L, Li M, Johanning L. Experimental investigation on the hydrodynamic

performance of a multi-chamber OWC-breakwater. Renewable and Sustainable Energy Reviews. 2021;150:111512.

[16] Zhao X, Li F, Zhou J, Geng J, Zou Q, Qin D. Theoretical investigation of hydrodynamic performance of multi-resonant OWC breakwater array. Appl Ocean Res. 2023;141:103756.

[17] Ding J, Pang S, Chen Z. Optimization of the chamber of OWC to improve hydrodynamic performance. Ocean Eng. 2023;287:115782.

[18] Gadelho JFM, Rezanejad K, Guedes Soares C, Santos JA, Anastas G, Fortes CJEM. Experimental study of an onshore dual chamber oscillating water column device. Ocean Eng. 2024;300:117240.

[19] Zhao X, Zou Q, Geng J, Zhang Y, Wang Z. Influences of wave resonance on hydrodynamic efficiency and loading of an OWC array under oblique waves. Appl Ocean Res. 2022;120:103069.

[20] Stansby P, Carpintero Moreno E, Stallard T, Maggi A. Three-float broad-band resonant line absorber with surge for wave energy conversion. Renew Energy. 2015;78:132-40.

[21] Stansby P, Carpintero Moreno E, Stallard T. Large capacity multi-float configurations for the wave energy converter M4 using a time-domain linear diffraction model. Appl Ocean Res. 2017;68:53-64.

[22] Liao Z, Stansby P, Li G. A generic linear non-causal optimal control framework integrated with wave excitation force prediction for multi-mode wave energy converters with application to M4. Appl Ocean Res. 2020;97:102056.

[23] Lande-Sudall DR, Nyland J, Rykkje TR, Stansby PK, Impelluso T. Hydrodynamic modelling of a multi-body wave energy converter using the Moving Frame Method. Mar Struct. 2023;87:103332.

[24] Cheng Y, Fu L, Dai S, Collu M, Cui L, Yuan Z, et al. Experimental and numerical analysis of a hybrid WEC-breakwater system combining an oscillating water column and an oscillating buoy. Renewable and Sustainable Energy Reviews. 2022;169:112909.

[25] Cui L, Zheng S, Zhang Y, Miles J, Iglesias G. Wave power extraction from a hybrid oscillating water column-oscillating buoy wave energy converter. Renewable and Sustainable Energy Reviews. 2021;135:110234.

[26] Wan C, Yang C, Bai X, Bi C, Chen H, Li M, et al. Numerical investigation on the hydrodynamics of a hybrid OWC wave energy converter combining a floating buoy. Ocean Eng. 2023;281:114818.

[27] Rashidi S, Nikseresht AH. Numerical investigation of the response of the hybrid wave energy converter including oscillating water column and horizontal floating cylinder to irregular waves. Energy. 2024;301:131717.

[28] Zhang C, Ning D. Hydrodynamic study of a novel breakwater with parabolic openings for wave energy harvest. Ocean Eng. 2019;182:540-51.

[29] Mayon R, Ning DZ, Zhang CW, Chen LF, Wang RQ. Wave energy capture by an omnidirectional point sink oscillating water column system. Appl Energy. 2021;304.

[30] Mayon R, Ning D, Sun Y, Ding Z, Wang R, Zhou Y. Experimental investigation on a novel and hyper-efficient oscillating water column wave energy converter coupled with a parabolic breakwater. Coastal Engineering. 2023;185:104360.

[31] Mayon R, Ning D, Xu J, Fu L. Oscillating water column wave energy converter arrays coupled with a parabolic-wall energy concentrator in regular and irregular wave conditions. Coastal Engineering. 2024;192:104559.

[32] Zhou B, Wang Y, Zheng Z, Jin P, Ning D. Power generation and wave attenuation of a hybrid system involving a heaving cylindrical wave energy converter in front of a parabolic breakwater. Energy. 2023;282:128364.

[33] Yu D, Wang KY, Liu HX, Kong FK, Yang C, Duan YP, et al. Investigation on motion

characteristics of an Anti-pitching Generating WEC (AGWEC) considering the viscous effect. Ocean Eng. 2022;246:17.
[34] Cheng Y, Liu W, Dai S, Yuan Z, Incecik A. Wave energy conversion by multi-mode exciting wave energy converters arrayed around a floating platform. Energy. 2024;313:133621.
[35] Jin SY, Wang DM, Hann M, Collins K, Conley D, Greaves D. A designed two-body hinged raft wave energy converter: From experimental study to annual power prediction for the EMEC site using WEC-Sim. Ocean Eng. 2023;267:16.
[36] Iturrioz A, Guanche R, Lara JL, Vidal C, Losada IJ. Validation of OpenFOAM® for Oscillating Water Column three-dimensional modeling. Ocean Eng. 2015;107:222-36.

Declaration of Competing Interest

The authors declare that they have no known competing financial interests or personal relationships that could have appeared to influence the work reported in this paper.